Turkish Journal of Physics

http://journals.tubitak.gov.tr/physics/

Research Article

Turk J Phys
(2018) 42: 600 – 612
© TÜBİTAK
doi:10.3906/fiz-1804-11

An analytic solution to the spin flavor precession for solar Majorana neutrinos in the case of three neutrino generations

Deniz YILMAZ*
Department of Physics Engineering, Faculty of Engineering, Ankara University, Ankara, Turkey

Received: 09.04.2018 • **Accepted/Published Online:** 03.09.2018 • **Final Version:** 12.10.2018

Abstract: The spin flavor precession (SFP) is investigated in the three neutrino generation case assuming that the neutrinos are of Majorana type. Approximate analytical formulas including all transition magnetic moments are provided for the electron neutrino survival probability and $\nu_e \to \overline{\nu}_e$ transition probability in the SFP framework. The accuracy of the formulas is checked for two different magnetic field profiles in the Sun.

Key words: Neutrino, Majorana, sprin flavor precession

1. Introduction

The combined analysis of the solar neutrino experiments [1–8] and reactor antineutrino experiment [9,10] established to confirm the neutrino oscillation strongly indicates the so-called large mixing angle (LMA) region of the neutrino parameter space [11–16]. In a minimal extension of the standard model, neutrinos have mass; hence, they also have magnetic moment. In addition to the limits on the neutrino magnetic moments obtained by experimental and theoretical studies [17–23], an upper bound was recently obtained by GEMMA experiments: $\mu_\nu < 2.9 \times 10^{-11} \mu_B$ at 90% CL [24]. One can also find detailed analyses and discussions on neutrino magnetic moment in the literature [25–31]. When neutrinos having nonzero magnetic moment propagate in a magnetic field, their spin can flip. Thus, a left handed neutrino becomes a right handed neutrino, $\nu_{e_L} \to \nu_{e_R}$, which is deliberated as a possible solution to the solar neutrino deficit [32]. When the matter effect is included, then a left handed neutrino becomes right handed another type of neutrino: $\nu_{e_L} \to \nu_{\mu_R}$ or ν_{τ_R} [33]. As distinct from the Dirac case in which right handed neutrino is considered as sterile which is not detectable by detectors, in the Majorana case, right handed neutrino is called antineutrino which can be detectable. This mechanism, called spin flavor precession (SFP), has been studied in different aspects [34–47]. In addition to the neutrino magnetic moment, a magnetic field profile in the Sun has to be chosen in order to carry out the SFP analysis quantitatively. The strength of the magnetic field in the Sun is limited by the standard solar model [48,49] such as $\sim$20 G near the solar surface [50], 20–300 kG at the convective zone [48] and $< 10^7$ G at the solar center [48]. In this study, two plausible profiles are considered as given in [51]; the first one is of the Gaussian type having a peak at the bottom of the convective zone (Figure 1a) and the second one is of the Woods–Saxon type being maximal at the centre of the Sun (Figure 1b).

In this paper, the SFP effect is studied in the case of three neutrino generations assuming that the neutrinos are of Majorana type and the approximate analytical formula including all neutrino parameters and

*Correspondence: dyilmaz@eng.ankara.edu.tr

This work is licensed under a Creative Commons Attribution 4.0 International License.

all types of neutrino magnetic moments is provided for the electron neutrino survival probability and $\nu_e \to \overline{\nu}_e$ transition probability. The accuracy of the formula is checked at different θ_{12}, δm^2_{12} values and for two different magnetic field profiles in the Sun. In Section 2, the formalism of the SFP mechanism is examined for the three neutrino generations. The deduction of the approximate analytical formulas are given in Sections 3 and 4. Results and conclusion are presented in the last section.

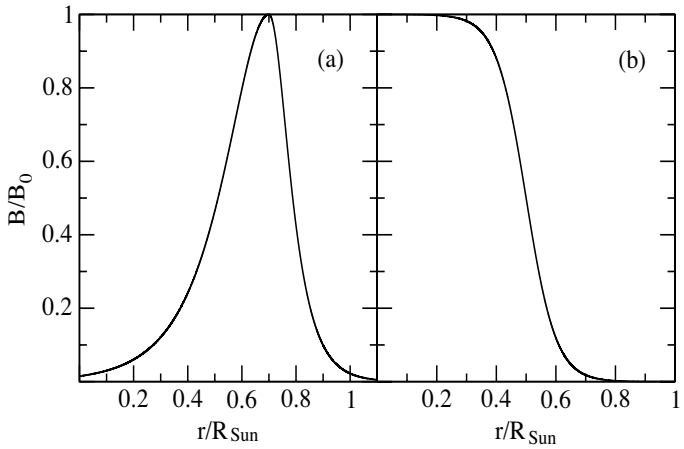

Figure 1. Magnetic field profiles: (a) Gaussian shape; (b) Woods–Saxon shape.

2. Spin flavor precession for the three neutrino generations

In the case of three neutrino generations, the evolution equation for Majorana neutrinos passing through the matter and the magnetic field can be generated by using 6×6 rotational matrices consisting of the 3×3 standard PMNS (Pontecorvo, Maki, Nakata, Sakata) mixing matrix [52]:

$$T_{12} = \begin{pmatrix} R_{12} & 0 \\ 0 & R_{12} \end{pmatrix}, \quad T_{13} = \begin{pmatrix} R_{13} & 0 \\ 0 & R_{13} \end{pmatrix}, \quad T_{23} = \begin{pmatrix} R_{23} & 0 \\ 0 & R_{23} \end{pmatrix}. \tag{1}$$

Here,

$$R_{23}R_{13}R_{12} = \begin{pmatrix} 1 & 0 & 0 \\ 0 & c_{23} & s_{23} \\ 0 & -s_{23} & c_{23} \end{pmatrix} \begin{pmatrix} c_{13} & 0 & s_{13}e^{-i\delta} \\ 0 & 1 & 0 \\ -s_{13}e^{i\delta} & 0 & c_{13} \end{pmatrix} \begin{pmatrix} c_{12} & s_{12} & 0 \\ -s_{12} & c_{12} & 0 \\ 0 & 0 & 1 \end{pmatrix}, \tag{2}$$

where $c_{ij} = cos\theta_{ij}$ and $s_{ij} = sin\theta_{ij}$ and the δ is the CP-violating phase that we will ignore in our discussion. Hereafter, we will use some useful abbreviations such as:

$$\begin{aligned} s^2_{ij} = sin^2\theta_{ij}, \qquad & c^2_{ij} = cos^2\theta_{ij}, \\ s2_{ij} = sin(2\theta_{ij}), \qquad & c2_{ij} = cos(2\theta_{ij}), \\ \Delta_{ij} = \frac{\delta m^2_{ij}}{2E}. & \end{aligned} \tag{3}$$

By taking Ψ and $\overline{\Psi}$ as

$$\Psi = \begin{pmatrix} \psi_e \\ \psi_\mu \\ \psi_\tau \end{pmatrix}, \quad \overline{\Psi} = \begin{pmatrix} \overline{\psi}_e \\ \overline{\psi}_\mu \\ \overline{\psi}_\tau \end{pmatrix}, \tag{4}$$

the evolution equation for Majorana neutrinos passing through the matter and the magnetic field can be written as

$$i\frac{d}{dt}\begin{pmatrix}\Psi\\ \overline{\Psi}\end{pmatrix}=\left[T_{23}T_{13}T_{12}\begin{pmatrix}E&0\\0&E\end{pmatrix}T_{12}^{\dagger}T_{13}^{\dagger}T_{23}^{\dagger}+\begin{pmatrix}V&0\\0&-V\end{pmatrix}+\begin{pmatrix}0&BM\\-BM&0\end{pmatrix}\right]\begin{pmatrix}\Psi\\ \overline{\Psi}\end{pmatrix}, \tag{5}$$

where E, V, and M are the 3×3 submatrices:

$$E=\begin{pmatrix}E_1&0&0\\0&E_2&0\\0&0&E_3\end{pmatrix},\ V=\begin{pmatrix}V_c+V_n&0&0\\0&V_n&0\\0&0&V_n\end{pmatrix},\ M=\begin{pmatrix}0&\mu_{e\mu}&\mu_{e\tau}\\-\mu_{e\mu}&0&\mu_{\mu\tau}\\-\mu_{e\tau}&-\mu_{\mu\tau}&0\end{pmatrix}. \tag{6}$$

Here, μ_{ij} is the transition magnetic moment (i and j denote the e, μ, τ). The evolution equation we obtain is

$$i\frac{d}{dt}\begin{pmatrix}\varphi\\ \overline{\varphi}\end{pmatrix}=\mathscr{H}\begin{pmatrix}\varphi\\ \overline{\varphi}\end{pmatrix}. \tag{7}$$

Here,

$$\varphi=\begin{pmatrix}\varphi_e\\ \varphi_\mu\\ \varphi_\tau\end{pmatrix}=\begin{pmatrix}c_{13}\psi_e-s_{13}\tilde{\psi}_\tau\\ \tilde{\psi}_\mu\\ s_{13}\psi_e+c_{13}\tilde{\psi}_\tau\end{pmatrix} \tag{8}$$

and

$$\begin{aligned}\tilde{\psi}_\mu&=c_{23}\psi_\mu-s_{23}\psi_\tau,\\ \tilde{\psi}_\tau&=s_{23}\psi_\mu+c_{23}\psi_\tau.\end{aligned} \tag{9}$$

Identical expressions are true for antineutrinos (just put a bar above). In the evalution equation above, $\mathscr{H}$ is

$$\mathscr{H}=\begin{pmatrix}H&BM'\\-BM'&\overline{H}\end{pmatrix}. \tag{10}$$

Here, after we have substracted off overall phase from the Hamiltonian; H, $\overline{H}$, and M' are

$$H=\begin{pmatrix}\frac{1}{2}\left(c_{13}^2V_c-c2_{12}\Delta_{21}\right)&\frac{s2_{12}\Delta_{21}}{2}&c_{13}s_{13}V_c\\ \frac{s2_{12}\Delta_{21}}{2}&\frac{1}{2}\left(-c_{13}^2V_c+c2_{12}\Delta_{21}\right)&0\\ c_{13}s_{13}V_c&0&V_c-\frac{3c_{13}^2V_c}{2}+\frac{1}{2}\left(\Delta_{31}+\Delta_{32}\right)\end{pmatrix}, \tag{11}$$

$$\overline{H}=\begin{pmatrix}D_{11}&\frac{1}{2}s2_{12}\Delta_{21}&-c_{13}s_{13}V_c\\ \frac{1}{2}s2_{12}\Delta_{21}&D_{22}&0\\ -c_{13}s_{13}V_c&0&D_{33}\end{pmatrix} \tag{12}$$

together with the diagonal elements

$$\begin{aligned}D_{11}&=-\tfrac{3}{2}c_{13}^2V_c-2V_n-\tfrac{1}{2}c2_{12}\Delta_{21},\\ D_{22}&=-\tfrac{1}{2}c_{13}^2V_c-2V_n+\tfrac{1}{2}c2_{12}\Delta_{21},\\ D_{33}&=\tfrac{1}{2}\left(-2+c_{13}^2\right)V_c-2V_n+\tfrac{1}{2}\left(\Delta_{31}+\Delta_{32}\right)\end{aligned} \tag{13}$$

and

$$M'=\begin{pmatrix}0&\mu_{12}&\mu_{13}\\-\mu_{12}&0&\mu_{23}\\-\mu_{13}&-\mu_{23}&0\end{pmatrix}. \tag{14}$$

Here, we defined

$$\begin{aligned}\mu_{12} &= c_{13}c_{23}\mu_{e\mu} - c_{13}s_{23}\mu_{e\tau} + s_{13}\mu_{\mu\tau},\\ \mu_{13} &= s_{23}\mu_{e\mu} + c_{23}\mu_{e\tau},\\ \mu_{23} &= -c_{23}s_{13}\mu_{e\mu} + s_{13}s_{23}\mu_{e\tau} + c_{13}\mu_{\mu\tau}.\end{aligned} \tag{15}$$

The matter potentials for the charged and the neutral current are given by

$$\begin{aligned}V_c &= \sqrt{2}G_F N_e,\\ V_n &= -\tfrac{G_F}{\sqrt{2}}N_n.\end{aligned} \tag{16}$$

Here, G_F is the Fermi constant and N_e and N_n are electron and neutron densities, respectively.

3. Deduction of the electron neutrino survival probability

We start with the evolution equation obtained in Section 2 for Majorana neutrinos passing through the matter and the magnetic field:

$$i\frac{d}{dt}\begin{pmatrix}\varphi\\ \overline{\varphi}\end{pmatrix} = \mathscr{H}\begin{pmatrix}\varphi\\ \overline{\varphi}\end{pmatrix}. \tag{17}$$

Here, φ and $\overline{\varphi}$ denote the three neutrino and antineutrino flavor parts, respectively. The matrix of $\mathscr{H}$ can be split into two parts as matter and magnetic parts:

$$\mathscr{H} = \mathscr{H}_M + \mathscr{H}_B. \tag{18}$$

Here, $\mathscr{H}_M$ and $\mathscr{H}_B$ are

$$\mathscr{H}_M = \begin{bmatrix} H & 0\\ 0 & \overline{H}\end{bmatrix}, \tag{19}$$

$$\mathscr{H}_B = \begin{bmatrix} 0 & BM'\\ -BM' & 0\end{bmatrix}. \tag{20}$$

We are going to solve the three-by-three blocks and use these solutions to solve the six-by-six matrix later.

Since the upper diagonal part of $\mathscr{H}_M$ is related to the neutrinos, the evolution equation for the neutrinos is

$$i\frac{d}{dt}\begin{pmatrix}\varphi_e\\ \varphi_\mu\\ \varphi_\tau\end{pmatrix} = H\begin{pmatrix}\varphi_e\\ \varphi_\mu\\ \varphi_\tau\end{pmatrix}. \tag{21}$$

Let us split H into two parts as well:

$$H = H^0 + H^1. \tag{22}$$

Here, H^0 is

$$H^0 = \begin{pmatrix} \frac{1}{2}\left(c_{13}^2V_c - c2_{12}\Delta_{21}\right) & \frac{s2_{12}\Delta_{21}}{2} & 0\\ \frac{s2_{12}\Delta_{21}}{2} & \frac{1}{2}\left(-c_{13}^2V_c + c2_{12}\Delta_{21}\right) & 0\\ 0 & 0 & b\end{pmatrix}, \tag{23}$$

where b is

$$b = V_c - \frac{3c_{13}^2V_c}{2} + \frac{1}{2}\left(\Delta_{31} + \Delta_{32}\right). \tag{24}$$

The evolution operator U_H for H satisfies the equation

$$i\frac{d}{dt}U_H = HU_H. \tag{25}$$

The solution to this equation can be sought by taking $U_H = U_H^0 U_H^1$. Since the equation $i\frac{d}{dt}U_H^0 = H^0 U_H^0$ associated with H^0 is the standard 2×2 MSW equation with an independent third flavor, the solution can be chosen as

$$U_H^0 = \begin{pmatrix} \psi_1 & -\psi_2^* & 0 \\ \psi_2 & \psi_1^* & 0 \\ 0 & 0 & \beta \end{pmatrix}, \tag{26}$$

where $\psi_1(t)$, $\psi_2(t)$ are 2×2 MSW solutions with the initial conditions $\psi_1(t=0)=1$, $\psi_2(t=0)=0$ [11] and β is

$$\beta = e^{-i\int b\,dt}. \tag{27}$$

We now can find the complete solution to all of H by looking at H^1:

$$i\frac{\partial U_H^1}{\partial t} = {U_H^0}^\dagger H^1 U_H^0 U_H^1 = h(t)U_H^1. \tag{28}$$

Because θ_{13} is small, we can apply an approximation to the solution of this equation:

$$U_H^1 = exp(-i\int_0^t h(t')dt') = \left[1 - i\int_0^t h(t')dt' - \frac{1}{2}\int_0^t\int_0^{t'} h(t')h(t'')dt'dt'' + ...\right] \tag{29}$$

Then we have the whole solution for H

$$U_H = U_H^0 U_H^1. \tag{30}$$

The antineutrino part of $\mathscr{H}_M$, $\overline{H}$, can be similarly solved. After $\overline{U}_{\overline{H}}$ is obtained, the solution matrix for the $\mathscr{H}_M$ can be written as:

$$U_M = \begin{bmatrix} U_H & 0 \\ 0 & \overline{U}_{\overline{H}} \end{bmatrix}. \tag{31}$$

Since the total evolution is characterized by $U = U_M U_B$, we need U_B which is the solution matrix of $\mathscr{H}_B$. By using the equation satisfied by the evolution operator of $\mathscr{H}$

$$i\frac{d}{dt}U = \mathscr{H}U, \tag{32}$$

we can get

$$i\frac{d}{dt}U_B = (U_M^\dagger \mathscr{H}_B U_M)U_B = h_b(t)U_B. \tag{33}$$

Because μB is small, U_B can also be found by applying an approximation up to the second order in μB

$$U_B = \left[1 - i\int_0^t h_b(t')dt' - \frac{1}{2}\int_0^t\int_0^{t'} h_b(t')h_b(t'')dt'dt'' + ...\right]. \tag{34}$$

The state of the system evolves with a unitary operator from the initial state

$$\begin{pmatrix} \varphi(t) \\ \overline{\varphi}(t) \end{pmatrix} = U \begin{pmatrix} \varphi(t=0) \\ \overline{\varphi}(t=0) \end{pmatrix} \tag{35}$$

with

$$U = U_M U_B = \begin{pmatrix} \mathrm{A} & \mathrm{C} \\ \mathrm{D} & \mathrm{B} \end{pmatrix}, \tag{36}$$

where A, B, C, and D are 3×3 matrices. The electron neutrino amplitude can be written from Eq. (8) as

$$\psi_e = c_{13}\varphi_e + s_{13}\varphi_\tau, \tag{37}$$

Since the elements of $\overline{\varphi}(t)$ at $t = 0$ is zero, it is enough to look at the A matrix only to obtain φ_e and φ_τ.

$$\begin{pmatrix} \varphi_e \\ \varphi_\mu \\ \varphi_\tau \end{pmatrix} = \begin{pmatrix} A_{11} & A_{12} & A_{13} \\ A_{21} & A_{22} & A_{23} \\ A_{31} & A_{32} & A_{33} \end{pmatrix} \begin{pmatrix} c_{13} \\ 0 \\ s_{13} \end{pmatrix}. \tag{38}$$

Therefore, one can find

$$\begin{aligned} \varphi_e &= A_{11}c_{13} + A_{13}s_{13}, \\ \varphi_\tau &= A_{31}c_{13} + A_{33}s_{13}. \end{aligned} \tag{39}$$

The highly oscillating integrations coming out in the solution matrix elements are ignored. However, stationary phase approximation method [53] can be used for the other integrals in which the SFP resonance width is considerably small as mentioned in [42]. After the terms that have higher order than s_{13}^2 are ignored, only A_{11}, A_{31}, and A_{33} matrix elements are left:

$$\begin{aligned} A_{11} &= \psi_1(t)\left(1 - \tfrac{1}{4}\tfrac{2\pi\Gamma_{\mu B}^2}{|d(\chi-2\kappa)/dt|_{(\chi-2\kappa)=0}}|\psi_1(t_R)|^2\right), \\ A_{31} &= -ic_{13}s_{13}e^{-i\int_0^t b\,dt'}\int_0^t dt' V_c(t')e^{i\int_0^{t'} b\,dt''}\psi_1(t'), \\ A_{33} &= e^{-i\int_0^t b\,dt'}. \end{aligned} \tag{40}$$

Here,

$$\begin{aligned} \Gamma_{\mu B} &= \mu_{eff}B, \\ \mu_{eff} &= c_{13}c_{23}\mu_{e\mu} - c_{13}s_{23}\mu_{e\tau} + s_{13}\mu_{\mu\tau}, \\ \kappa &= \tfrac{\Delta_{21}}{2}c2_{12}, \\ \chi &= \tfrac{G_f}{\sqrt{2}}\left(2N_e - 2N_n\right). \end{aligned} \tag{41}$$

Substituting φ_e and φ_τ and the terms A_{11}, A_{31}, and A_{33} into ψ_e, we obtain

$$\begin{aligned} \psi_e = \psi_1(t)c_{13}^2 &\left(1 - \tfrac{1}{4}\tfrac{2\pi\Gamma_{\mu B}^2}{|d(\chi-2\kappa)/dt|_{(\chi-2\kappa)=0}}|\psi_1(t_R)|^2\right) \\ &-ic_{13}^2s_{13}^2e^{-i\int_0^t b\,dt'}\int_0^t dt' V_c(t')e^{i\int_0^{t'} b\,dt''}\psi_1(t') + s_{13}^2e^{-i\int_0^t b\,dt'}. \end{aligned} \tag{42}$$

Here, the integral can be solved by using the same method given in [11].

One can finally get the electron survival probability for three neutrino generations in the SFP framework by ignoring the terms that have higher order than $(\mu B)^2$

$$P_{3\times3}(\nu_e \to \nu_e, \mu B \neq 0) = c_{13}^4 P_{2\times2}(\nu_e \to \nu_e \ \text{ with } \ N_e c_{13}^2, \mu B = 0) \left(1 - \frac{1}{2} \frac{2\pi\Gamma_{\mu B}^2}{|d(\chi - 2\kappa)/dt|_{(\chi-2\kappa)=0}} |\psi_1(t_R)|^2\right) + s_{13}^4 \left[1 + 2\xi c_{13}^2 + \xi^2 c_{13}^4\right], \tag{43}$$

where

$$\xi = \frac{V_c(t=0)}{\Delta_{31}}. \tag{44}$$

4. Analytical expression for $\nu_e \to \overline{\nu}_e$ transition probability

If the neutrinos are assumed to be of Majorana type, ν_e changes to $\overline{\nu}_{\mu,\tau}$ inside the Sun by SFP. After the Sun, $\overline{\nu}_{\mu,\tau}$ transforms to $\overline{\nu}_e$ via vacuum oscillation:

$$\nu_e \overset{SFP}{\to} \overline{\nu}_{\mu,\tau} \overset{V_{osc}}{\to} \overline{\nu}_e.$$

Hence, the electron antineutrino flux, $\Phi_{\overline{\nu}_e}(E)$, on Earth is given by

$$\Phi_{\overline{\nu}_e}(E) = \Phi_{\nu_e}(E) \times P(\nu_e \to \overline{\nu}_e), \tag{45}$$

where $\Phi_{\nu_e}(E)$ is the solar electron neutrino flux with energy E. Therefore, one needs the $\nu_e \to \overline{\nu}_e$ transition probability to find the electron antineutrino flux on Earth:

$$P(\nu_e \to \overline{\nu}_e) = P(\nu_e \to \overline{\nu}_{\mu,\tau}; SFP) \times P(\overline{\nu}_{\mu,\tau} \to \overline{\nu}_e; VacuumOsc.). \tag{46}$$

Here, $P(\overline{\nu}_{\mu,\tau} \to \overline{\nu}_e; VacuumOsc.)$ is the well known vacuum oscillation probability given as

$$P(\overline{\nu}_{\mu,\tau} \to \overline{\nu}_e; VacuumOsc.) = sin^2\theta_{12} sin^2\left(\frac{\delta m_{12}^2}{4E} R\right) \overset{averaging}{\to} \frac{1}{2} sin^2\theta_{12} \tag{47}$$

and $P(\nu_e \to \overline{\nu}_{\mu,\tau}; SFP)$ is the $\nu_e \to \overline{\nu}_{\mu,\tau}$ transition probability:

$$P(\nu_e \to \overline{\nu}_{\mu,\tau}; SFP) = |\ \overline{\psi}_{\mu,\tau}|^2. \tag{48}$$

Here, $\overline{\psi}_{\mu,\tau}$ can be found with the solution of antineutrino part in Eq. (19) by using the same method given in Section 3:

$$\overline{\psi}_\mu = -ic_{13} \left(\frac{2\pi\Gamma_{\mu B}^2}{|d(\chi - 2\kappa)/dt|_{(\chi-2\kappa)=0}}\right)^{1/2} \psi_1(t_R) \overline{\psi}_2(t_R) \left(c_{23} \overline{\psi}_1^*(t) + s_{23} s_{13} \overline{\psi}_2^*(t)\right) \tag{49}$$

and

$$\overline{\psi}_\tau = \overline{\psi}_\mu (c_{23} \to -s_{23},\ s_{23} \to c_{23}). \tag{50}$$

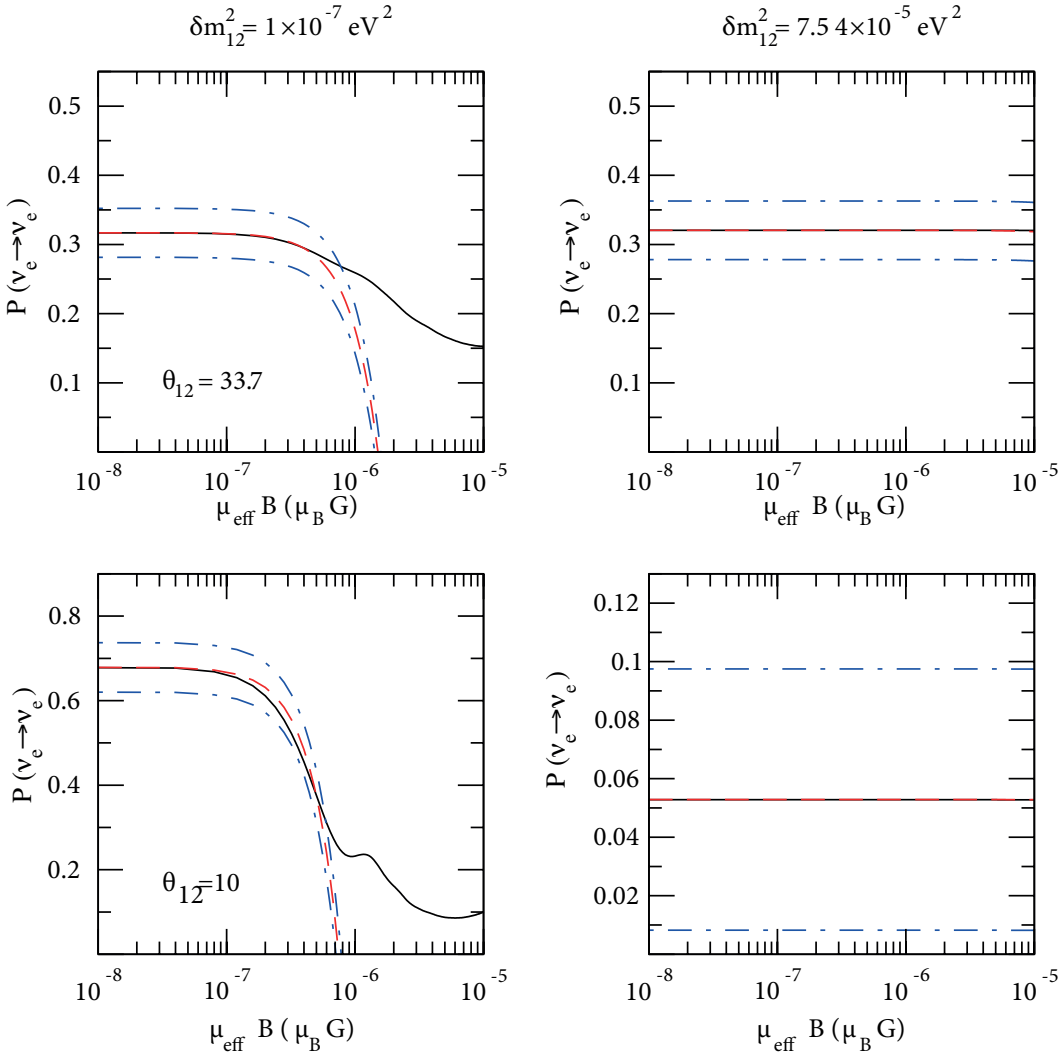

Figure 2. Survival probabilities for the 10 MeV neutrino energy at different θ_{12} and δm^2_{12} values for the Gaussian shape of magnetic field profile. While the solid lines show the results obtained numerically, the dashed lines show the result obtained from the approximate analytical expression. The dotted-dashed lines show the errors. Each column (row) uses the same δm^2_{12} (θ_{12}) values.

5. Results and conclusions

In this paper, the SFP effect studied in 2-neutrino cases [54] was generalized to the more complex 3-neutrino cases and the $\nu_e \to \overline{\nu}_e$ transition probability was also analyzed. We examined the SFP mechanism in the three neutrino generations and obtained approximate analytical formulas including all neutrino parameters and all types of neutrino magnetic moments. It can be easily seen that the results obtained here is reduced to the 2-neutrino cases when the parameters related with the third neutrino flavor are taken to be zero. The accuracy of the approximate solution obtained by the formulas was checked by comparing it with the exact solution obtained numerically by diagonalizing the Hamiltonian in Eq. (7) for two different magnetic field profiles in the Sun. In the calculations, the Gaussian (Figure 1a) and the Woods–Saxon shape (Figure 1b) of magnetic field profiles extending over the entire Sun were chosen [51]. The figures (Figures 2–6) are plotted as a function of the

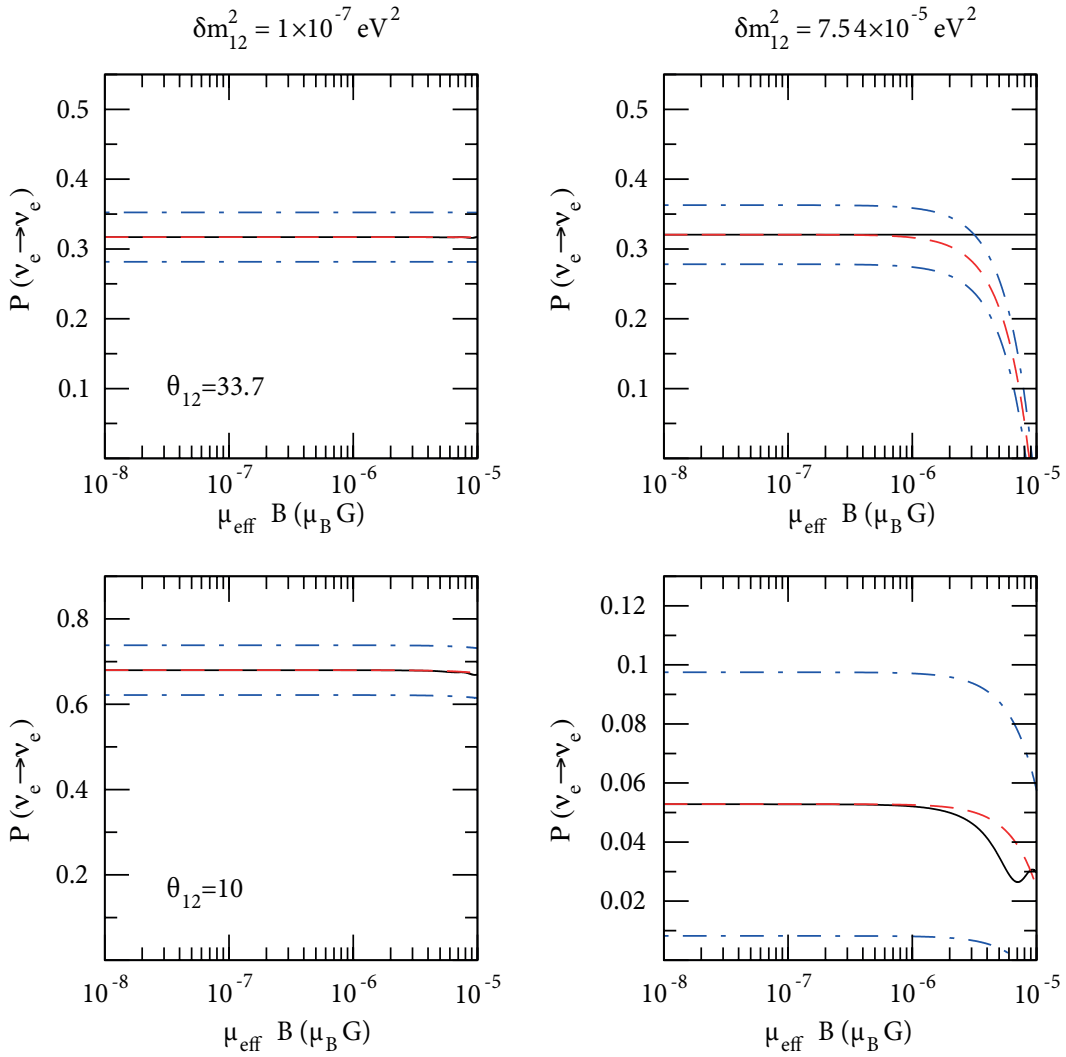

Figure 3. Survival probabilities for the 10 MeV neutrino energy at different θ_{12} and δm^2_{12} values for the Woods–Saxon shape of magnetic field profile. While the solid lines show the results obtained numerically, the dashed lines show the result obtained from the approximate analytical expression. The dotted-dashed lines show the errors. Each column (row) uses the same δm^2_{12} (θ_{12}) values.

product $\mu_{eff}B$, since μ_{eff} and B appeared together in the survival probability expression in Eq. (43). μ_{eff} given explicitly in Eq. (41) includes three transition magnetic moments with the upper bound $\mu_{ij} \lesssim 10^{-11}\mu_B$ (i and j denote e, μ, τ) [31]. Results are presented at different θ_{12}, δm^2_{12} values. The best fit values of all neutrino parameters and their errors are taken from [52].

Electron neutrino survival probabilities obtained by using exact (solid lines) and approximate solution (dashed lines) for the 10 MeV neutrino energy are shown in Figures 2 and 3 with the errors (dotted-dashed lines) for the Gaussian and the Woods–Saxon shape of magnetic field profiles, respectively. In these figures, one can see at what values of $\mu_{eff}B$ the approximate solution works well.

Figures 4 and 5 show the percent accuracy regions at different θ_{12} and δm^2_{12} values for the Gaussian and the Woods–Saxon shape of magnetic field profiles, respectively. In these figures, compared to the results

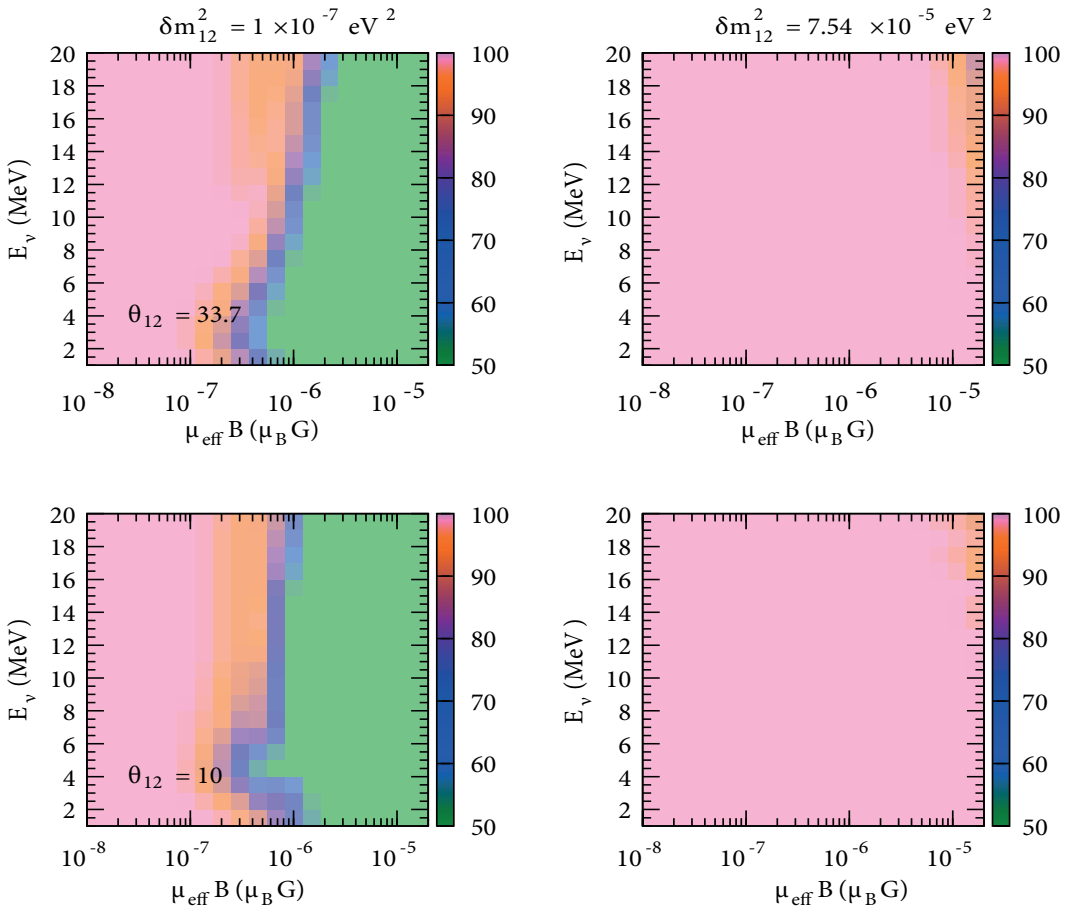

Figure 4. Percent accuracy regions at different θ_{12} and δm^2_{12} values for the Gaussian shape of magnetic field profile. The accuracy rates are given between 100% and 50%. Each column (row) uses the same δm^2_{12} (θ_{12}) values.

from the exact solution, how reliable the approximate analytical formula is shown. The accuracy rates are given between 100% and 50%. The results obtained from the formula are quite compatible with the exact solution results (almost in 99.9 percent accuracy) at $\delta m^2_{12} = 7.54 \times 10^{-5} eV^2$ for the Gaussian magnetic field profile and at $\delta m^2_{12} = 1 \times 10^{-7} eV^2$ for the Woods–Saxon magnetic field profile for almost all $\mu_{eff} B$ values and neutrino energies. Besides, for the MSW-LMA best fit values (upper right panels of each figures), we have 99.9 percent accuracy as well nearly up to the $1 - 2 \times 10^{-6} \mu_B G$ value of $\mu_{eff} B$ which is a sufficiently high value for the Sun at all neutrino energies for both magnetic field profiles. Additionally, it is seen that for $\delta m^2_{12} = 7.54 \times 10^{-5} eV^2$, the formula is also highly reliable at low neutrino energies even for high enough values of $\mu_{eff} B$.

In Figure 6, $\nu_e \to \overline{\nu}_e$ transition probabilities are shown for 2 MeV neutrino energy and at best fit LMA values of θ_{12} and δm^2_{12} for the Gaussian shape (a) and Woods–Saxon shape (b) of magnetic field profiles. It can be seen that the results obtained from the analytical expression (dashed lines) are compatible with the ones obtained numerically (solid lines) for both magnetic field profiles. This may allow the expression to be used in the calculations of the solar antineutrino flux on Earth.

In conclusion, even though the evolution equation can be solved numerically, one might need to have an approximated analytical solution to see the behaviour of the probabilities in SFP framework without performing

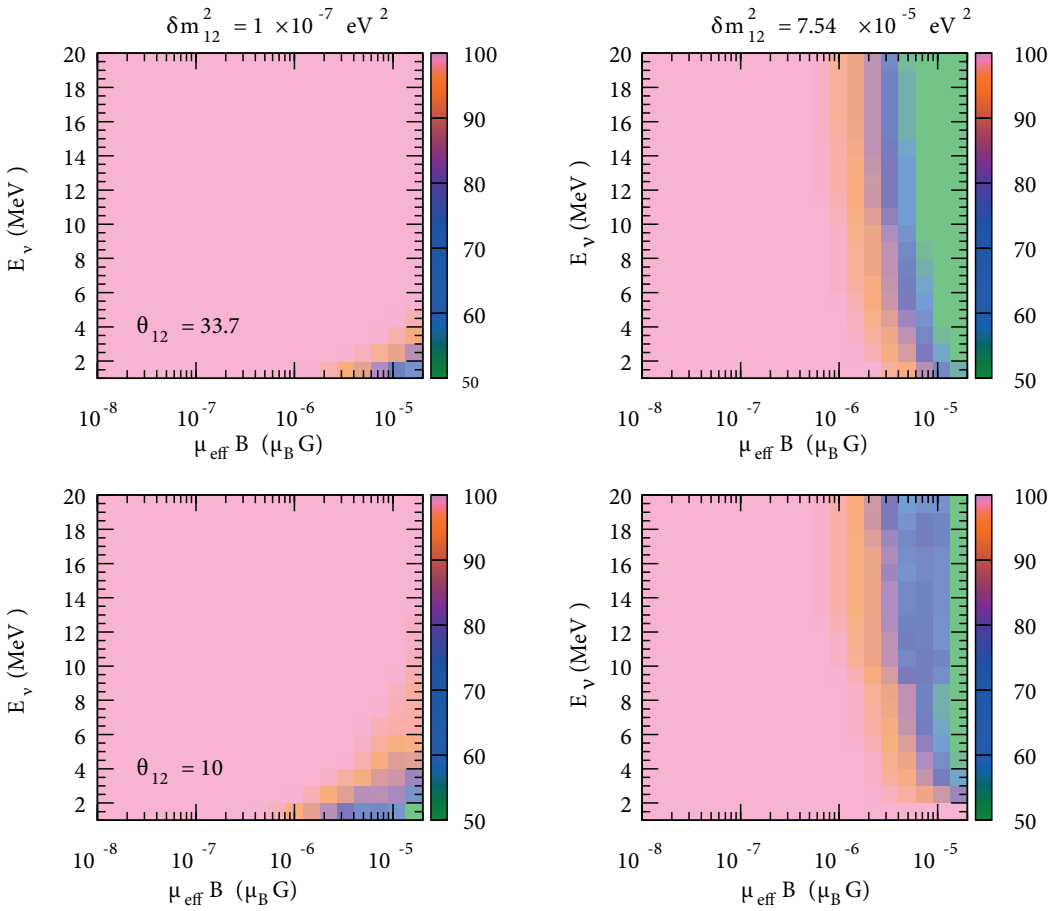

Figure 5. Percent accuracy regions at different θ_{12} and δm^2_{12} values for the Woods–Saxon shape of magnetic field profile. The accuracy rates are given between 100% and 50%. Each column (row) uses the same δm^2_{12} (θ_{12}) values.

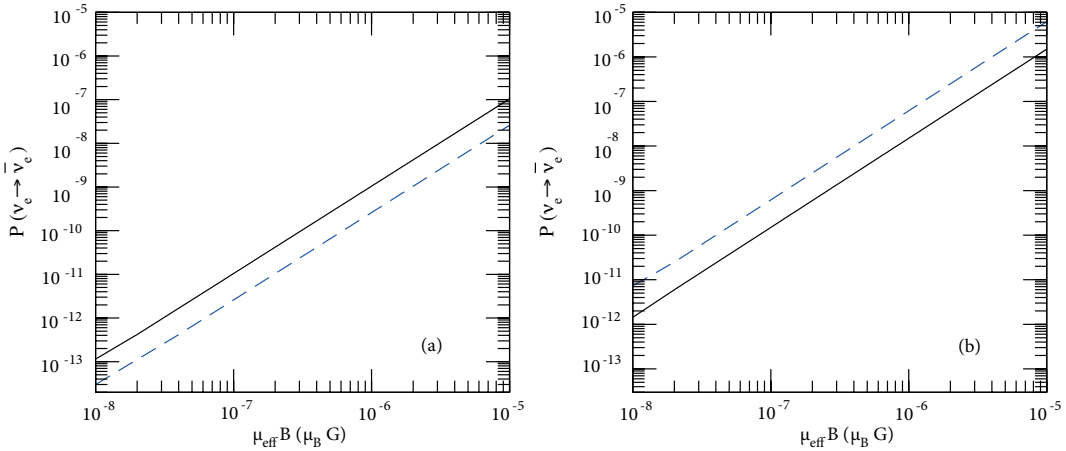

Figure 6. $\nu_e \to \overline{\nu}_e$ transition probabilities for 2 MeV neutrino energy and at best fit LMA values of θ_{12} and δm^2_{12} for the Gaussian shape (a) and Woods–Saxon shape (b) of magnetic field profiles. While the solid lines show the results obtained numerically, the dashed lines show the result obtained from the approximate analytical expression.

detailed numerical analysis. The dependence of the analytical probability expressions on the neutrino parameters can be seen from the expressions between Eqs. (43) and (50). Moreover, the formulas derived here can also be useful when the data obtained by new solar neutrino experiments is analyzed in the SFP framework.

Acknowledgments

I would like to thank A. Baha Balantekin and Annelise Malkus for the insightful discussions and their invaluable suggestions. I also thank YÖK (Council of Higher Education) for the grant to support my research at the University of Wisconsin, Madison.

References

[1] Ahmad, Q. R.; Allen, R. C.; Andersen, T. C.; Anglin, J. D.; Bühler, G.; Barton, J. C.; Beier, E. W.; Bercovitch, M.; Bigu, J.; Biller, S. et al. [SNO Collaboration], *Phys. Rev. Lett.* **2001**, *87*, 071301.

[2] Aharmim, B.; Ahmad, Q. R.; Ahmed, S. N.; Allen, R. C.; Andersen, T. C.; Anglin, J. D.; Bühler, G.; Barton, J. C.; Beier, E. W.; Bercovitch, M. et al. [SNO Collaboration], *Phys. Rev. C* **2007**, *75*, 045502.

[3] Fukuda, S.; Fukuda, Y.; Ishitsuka, M.; Itow, Y.; Kajita, T.; Kameda, J.; Kaneyuki, K.; Kobayashi, K.; Koshio, Y.; Miura, M. et al. [Super-Kamiokande Collaboration], *Phys. Rev. Lett.* **2001**, *86*, 5651–5655.

[4] Fukuda, S.; Fukuda, Y.; Ishitsuka, M.; Itow, Y.; Kajita, T.; Kameda, J.; Kaneyuki, K.; Kobayashi, K.; Koshio, Y.; Miura, M. et al. [Super-Kamiokande Collaboration], *Phys. Lett. B* **2002**, *539*, 179-187.

[5] Cleveland, B. T.; Daily, T.; Davis, R. Jr.; Distel, J. R.; Lande, K.; Lee, C. K.; Wildenhain, P. S.; Ullman, J. *Astrophys. J.* **1998**, *496*, 505-526.

[6] Abdurashitov, J. N.; Gavrin, V. N.; Girin, S. V.; Gorbachev, V. V.; Gurkina, P. P.; Ibragimova, T. V.; Kalikhov, A. V.; Khairnasov, N. G.; Knodel, T. V.; Mirnov, I. N. [SAGE Collaboration], *J. Exp. Theor. Phys.* **2002**, *95*, 181-193.

[7] Hampel, W.; Handt, J.; Heusser, G.; Kiko, J.; Kirsten, T.; Laubenstein, M.; Pernicka, E.; Rau, W.; Wojcik, M.;Zakharov, Y. et al. [GALLEX Collaboration], *Phys. Lett. B* **1999**, *447*, 127-133.

[8] Altmann, M.; Balata, M.; Belli, P.; Bellotti, E.; Bernabei, R.; Burkert, E.; Cattadori, C.; Cerichelli, G.; Chiarini, M.; Cribier, M. et al. [GNO Collaboration], *Phys. Lett. B* **2000**, *490*, 16-26.

[9] Eguchi, K.; Enomoto,S.; Furuno, K.; Goldman, J.; Hanada, H.; Ikeda, H.; Ikeda, K.; Inoue, K.;Ishihara, K.; Itoh, W. et al. [KamLAND Collaboration], *Phys. Rev. Lett.* **2003**, *90*, 021802.

[10] Araki, T.; Eguchi, K.; Enomoto, S.; Furuno, K.; Ichimura, K.; Ikeda, H.; Inoue, K.; Ishihara, K.; Iwamoto, T.; Kawashima, T. et al. [KamLAND Collaboration], *Phys. Rev. Lett.* **2005**, *94*, 081801 (1-5).

[11] Balantekin, A. B.; Yuksel, H. *J. Phys. G* **2003**, *29*, 665-682.

[12] Bahcall, J. N.; Pena-Garay, C. *J. High Energy Phys.* **2003**, *0311*, 004 (1-49).

[13] Gonzalez-Garcia, M. C.; Pena-Garay, C. *Phys. Rev. D* **2003**, *68*, 093003.

[14] de Holanda, P. C.; Smirnov, A. Y. *Phys. Rev. D* **2004**, *69*, 113002.

[15] Fogli, G. L.; Lisi, E.; Marrone, A.; Palazzo, A. *Phys. Lett. B* **2004**, *583*, 149-156.

[16] Bahcall, J. N.; Gonzalez-Garcia, M. C.; Pena-Garay, C. *J. High Energy Phys.* **2004**, *04008*, 016.

[17] Raffelt, G. G. *Phys. Rev. Lett.* **1990**, *64*, 2856-2858.

[18] Lattimer, J. M.; Cooperstein, J. *Phys. Rev. Lett.* **1988**, *61*, 23-26.

[19] Barbieri, R.; Mohapatra, R. N. *Phys. Rev. Lett.* **1988**, *61*, 27-30.

[20] Liu, D.W.; Ashie, Y.; Fukuda, S.; Fukuda, Y.; Ishihara, K.; Itow, Y.; Koshio, Y.; Minamino, A.; Miura, M.; Moriyama, S. et al. [Super-Kamiokande Collaboration], *Phys. Rev. Lett.* **2004**, *93*, 021802.

[21] Wong, H. T.; Li, H. B.; Lin, S. T.; Lee, F. S.; Singh, V.; Wu, S. C.; Chang, C. Y.; Chang, H. M.; Chen, C. P.; Chou, M. H. et al. [TEXONO Collaboration], *Phys. Rev. D* **2007**, *75*, 012001.

[22] Daraktchieva, Z.; Amsler, C.; Avenier, M.; Broggini, C.; Busto, J.; Cerna, C.; Juget, F.; Koang, D. H.; Lamblin, J.; Lebrun, D. et al. [MUNU Collaboration], *Phys. Lett. B* **2005**, *615*, 153-159.

[23] Papoulias, D. K.; Kosmas, T. S. *Phys. Lett. B* **2015**, *747*, 454-459.

[24] Beda, A. G.; Brudanin, V. B.; Egorov, V. G.; Medvedev, D. V.; Pogosov, V. S.; Shevchik, E. A.; Shirchenko, M. V.; Starostin, A. S.; Zhitnikov, I. V. *Phys. Part. Nucl. Lett.* **2013**, *10*, 139-143.

[25] Beacom, J. F.; Vogel, P. *Phys. Rev. Lett.* **1999**, *83*, 5222-5225.

[26] Bell, N. F.; Cirigliano, V.; Ramsey-Musolf, M. J.; Vogel,P.; Wise, M. B. *AIP Conf. Proc.* **2006**, *842* 874-846.

[27] Bell, N. F.; Gorchtein, M.; Ramsey-Musolf, M. J.; Vogel, P.; Wang, P. *Phys. Lett. B* **2006**, *642*, 377-383.

[28] Balantekin, A. B. *AIP Conf. Proc.* **2006**, *847*, 126-133.

[29] Studenikin, A. *Nucl. Phys. Proc. Suppl.* **2009**, *188*, 220-222.

[30] Broggini, C.; Giunti, C.; Studenikin, A.; *Adv. High Energy Phys.* **2012**, 459526.

[31] Vassh, N.; Grohs, E.; Balantekin, A. B.; Fuller, G. M. *Phys. Rev. D* **2015**, *92*, 125020

[32] Cisneros, A. *Astrophys. Space Sci.* **1971**, *10*, 87-92. doi:10.1007/BF00654607

[33] Lim, C. S.; Marciano, W. J. *Phys. Rev. D* **1988**, *37*, 1368.

[34] Okun, L. B.; Voloshin, M. B.; Vysotsky, M. I. *Sov. J. Nucl. Phys.* **1986**, *44*, 440, *Yad. Fiz.* **1986**, *44*, 677.

[35] Akhmedov, E. K. *Phys. Lett. B* **1988**, *213*, 64-68.

[36] Akhmedov, E. K.; Khlopov, M. Y. *Mod. Phys. Lett. A* **1988**, *3*, 451-457.

[37] Barbieri, R.; Fiorentini, R. *Nucl. Phys. B* **1988**, *304*, 909-920.

[38] Balantekin, A. B.; Hatchell, P. J.; Loreti, F. *Phys. Rev. D* **1990**, *41*, 3583-3593.

[39] Bykov, A. A.; Popov, V. Y.; Rashba, T. I.; Semikoz, V. B. arXiv:hep-ph/0002174.

[40] Akhmedov, E. K.; Pulido, J. *Phys. Lett. B* **2003**, *553*, 7-17.

[41] Chauhan, B. C.; Pulido, J; Torrente-Lujan, E. *Phys. Rev. D* **2003**, *68*, 033015.

[42] Balantekin, A. B.; Volpe, C. *Phys. Rev. D* **2005**, *72*, 033008.

[43] Yilmaz, D.; Yilmazer, A. U. *J. Phys. G* **2005**, *31*, 57-69.

[44] Yilmaz, D.; Yilmazer, A. U. *J. Phys. G* **2005**, *31*, 1123-1131.

[45] Yilmaz, D. *Adv. High Energy Phys.* **2016**, 1435191.

[46] Ando, S.; Sato, K. *Phys. Rev. D* **2003**, *67*, 023004. doi:10.1103/PhysRevD.67.023004

[47] Studenikin, A. *EPJ Web Conf.* **2016**, *125*, 04018.

[48] Couvidat, S.; Turck-Chieze, S.; Kosovichev, A. G. *Astrophys. J.* **2003**, *599*, 1434-1448.

[49] Bahcall, J. N.; Pinsonneault, M. H. *Phys. Rev. Lett.* **2004**, *92*, 121301.

[50] Antia, H. M.; Chitre, S. M.; Thompson, M. J. *Astron. Astrophys.* **2000**, *360*, 335-344.

[51] Das, C. R.; Pulido, J.; Picariello, M. *Phys. Rev. D* **2009**, *79*, 073010.

[52] Particle Data Group Collaboration, *Chin. Phys. C* **2014**, *38*, 090001.

[53] Balantekin, A. B.; Fetter, J. M.; Loreti, F. *Phys. Rev. D* **1996**, *54*, 3941.

[54] Yilmaz, D. *Turk. J. Phys.* **2014**, *38*, 187-192 . doi:10.3906/fiz-1401-13